CHINESE JOURNAL OF PHYSICS VOL. 38, NO. 2-II APRIL 2000

X-ray Structure Analysis of Bi2212 Using Synchrotron Source and High Dynamic Range Imaging Plate Detector

T. J. Lee[1], C. F. Huang[1], C. C. Teo[1], T. S Khor[1], H. C. Ku[1], K. W. Yeh[2], Y. Huang[2], H. H. Hung[3], Kiwako Sakabe[4], and Noriyoshi Sakabe[5]

[1]*Department of Physics, National Tsing Hua University, Hsinchu, Taiwan 300. R.O.C.*
[2]*Materials Science Center, National Tsing Hua University, Hsinchu, Taiwan 300, R.O.C.*
[3]*SRRC, Hsinchu, Taiwan 300, R.O.C.*
[4]*Department of Chemistry, Faculty of Science University of Nagoya, Nagoya 464, Japan*
[5]*Institute of Applied Biochemistry and Tsukuba Advanced Research Alliance (TARA), University of Tsukuba, Ibaraki 305, Japan*

(Received August 17, 1999)

The traveling solvent floating zone method was applied in growing the single crystals of $Bi_2Sr_2PrCu_2O_{8+\delta}$. Diffraction patterns of $0kl$, $1kl$, $2kl$, $3kl$, $4kl$ were obtained with the Weissenberg camera equipped with Fuji 400 imaging plate in Photon Factory, KEK. The wavelength of the photon is tuned to 1Å. With this energy, modulation peaks of "order 3" can be recorded clearly. From the extinction conditions in the diffraction pattern indicate the main structure of the crystal can be attributed to orthorhombic *Amaa*. Using oscillation photograph and zero level Weissenberg photograph, cell lengths of the crystal were calculated to be $\mathsf{a} = 5.489(2)$, $\mathsf{b} = 5.526(5)$, $\mathsf{c} = 30.420(7)$ Å. The crystal possesses an incommensurate modulation along b direction, with modulation wave vector $\mathbf{q} = 0.243\mathbf{b}^* + \mathbf{c}^*$ and can be expressed as super space group: N_{11}^{Amaa}.

PACS. 61. – Structure of solids.
PACS. 61.10.Nz – Single-crystal and powder diffraction.
PACS. 74.70.–h – High T_c compounds.

I. Introduction

The pursuit of understanding the modulated structures in high T_c superconductor started with the discovery of the $Bi_2Sr_2CaCu_2O_{8+\delta}$ phase in early 1988 [16]. One of the earliest structural studies by Subramanian *et al.* [23] and Gao *et al.* [6, 7] reported the observation of satellite reflection at $\sim (\pm 0.21\ \mathbf{b}^{\ddagger})$. Later on many researcher revealed that the Bi-based superconducting or non-superconducting materials have modulated structure, which are either similar to or more complicate than that of $Bi_2Sr_2CaCu_2O_{8+\delta}$ phase. In this work, single crystal of $Bi_2Sr_2PrCu_2O_{8+\delta}$ was investigated by Weissenberg method incorporated with the high intensity synchrotron X-ray in order to study both the main and modulated structure of this compound.

The crystallography of modulated structure is based on a superspace description developed by De Wolff, Janssen and Janner [3, 11, 12]. The modulation waves can involve atomic positions (displacive modulation), temperature factors, site occupancies (occupational modulation), spin

density or combinations of these. In a crystal with n independent modulation waves, (3+n)-dimensional superspace is used. For application to most bismuth-based superconductors, which we intend to study in this work, one-dimensional displacive modulation will be discussed here.

A modulation wave is defined in reciprocal space by a "wave vector" **q**:

$$\mathbf{q} = \alpha\mathbf{a}^{¤} + \beta\mathbf{b}^{¤} + \gamma\mathbf{c}^{¤}$$

where $\mathbf{a}^{¤}$, $\mathbf{b}^{¤}$ and $\mathbf{c}^{¤}$ define the basic lattice in the reciprocal space. If one or more of the coefficients α, β and γ are irrational, the modulation wavelength $\lambda_m = 1/|\mathbf{q}|$, is incommensurate with the basis lattice in that direction. Otherwise, the modulation wavelength is commensurate with the basic lattice.

The scattering vector **Q** in a one-dimensionally modulated crystal is the sum of the scattering vector **H**, defined by $(h, k, 1)$ the basic lattice and a multiple of the wave vector **q**:

$$\begin{aligned}\mathbf{Q} &= \mathbf{H} + m\mathbf{q} \\ &= h\mathbf{a}^{¤} + k\mathbf{b}^{¤} + l\mathbf{c}^{¤} + m\mathbf{q}.\end{aligned}$$

A reflection with $m = 0$ is referred to as a "main" reflection; a reflection with $m \neq 0$ is referred to as an m-th order "satellite" reflection. Therefore, a reflection in a one-dimensionally modulated crystal has a four indices: $h, k, 1, m$.

The incommensurate modulated structure of the high-temperature superconductor $Bi_2Sr_2CaCu_2O_{8+\delta}$ (Bi2212) has been the subject of intense study since its discovery by Maeda *et al*. [16]. Many X-ray diffraction [23, 27], electron diffraction [5] and neutron diffraction [9] studies have been undertaken to understand the intricate structure of this complex material. The averaged structure of this high-temperature superconducting compound was readily identiffed, however, the real structure turned out to be more complicated than expected, since it combines displacive and substitutive modulation.

The average structure of the compound $Bi_2Sr_2CaCu_2O_{8+\delta}$ has been reported by several authors in space group $Cccm$ [8] with the unit cell parameters $\mathbf{a} \approx \mathbf{c} \approx 5.4$Å and $\mathbf{b} \approx 30.74$Å. The later published works [24, 25, 26] on the isostructure of Bi-based compounds usually referring to the non-standard setting $Amaa$ by labeling the shortest translation as a, the intermediate translation as **b**, and the longest translation as **c**. Table I summarized the results in the past.

Though an enormous amount of data has generated by X-ray or neutron diffraction, electron diffraction, electron microscopy and other chemical measurements in the past decade, the structure and functional relation is not well established for $Bi_2Sr_2CaCu_2O_{8+\delta}$.

II. Experiments

II-1. Sample preparation

The bulk sample of $Bi_2Sr_2PrCu_2O_{8+\delta}$ is obtained by mixing Bi_2O_3, $Sr(CO_3)_2$, Pr_2O_3 and CuO powder in stochiometrical ratio, using sintering process. It was regranuated and pressed for several times while sintering, in order to improve the purity of Bi2212 phase. Schematic of thermal cycle employed for crystal growth is shown in Fig. 1.

TABLE I.

	a(Å)	**b**(Å)	**c**(Å)	**Q**
Miles *et al*., ILL, RT crystal [16]	5.388(4)	5.3880(4)	30.778(1)	0.210(2)
Miles *et al*., ILL, 12 K crystal [16]	5.3846(7)	5.3932(2)	30.622(3)	0.210(2)
Miles *et al*., 2TanA, crystal [16]	5.398(4)	5.399(4)	30.708(2)	0.210(2)
Miles *et al*., X-ray, powder [16]	5.3968(5)	5.401(1)	30.7982(5)	0.2088(2)
Miles *et al*., neutron, powder [16]	5.398(5)	5.401(1)	30.798(5)	0.209(2)
Fu *et al*., electron, crystal [4]	5.39	5.39	30.6	0.21
Beskrovnyi *et al*., neutron, crystal [1]	5.397(1)	5.401(1)	30.716(3)	0.21
Kan *et al*., X-ray, crystal [13]	5.415(2)	5.421(2)	30.88(2)	N/A
Petricek *et al*., X-ray, clystal [18]	5.408(1)	5.413(1)	30.871(5)	0.210(3)
Petricek *et al*., neutron, powder [18]	5.4149(3)	5.4150(3)	30.861(5)	0.2095
Yamamoto *et al*., X-ray, powder [28,29]	5.3957(3)	5.3971(3)	30.649(1)	0.2118(1)
Yamamoto *et a1*., neutron powder [28,29]	5.3957(3)	5.3971(3)	30.649(1)	0.2118(1)

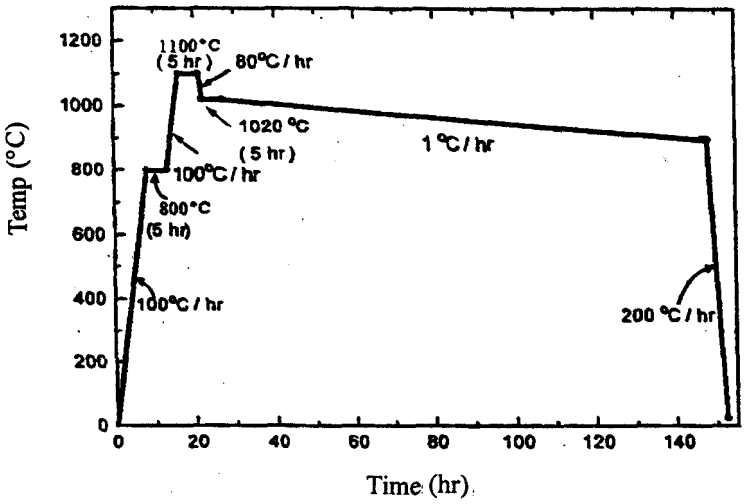

FIG. 1. Thermal cycle for preparation of bulk sample in the sintering process.

The bulk samples, which were obtained from the sintering process, were confirmed by powder X-ray diffraction pattern, Fig. 2, using JADE search match program [10] incorporated with the ICDD and ICSD databases. RUBY program package [10] was used to calculate the diffraction pattern and the corresponding Bragg's angles for the isostructure of the possible phase.

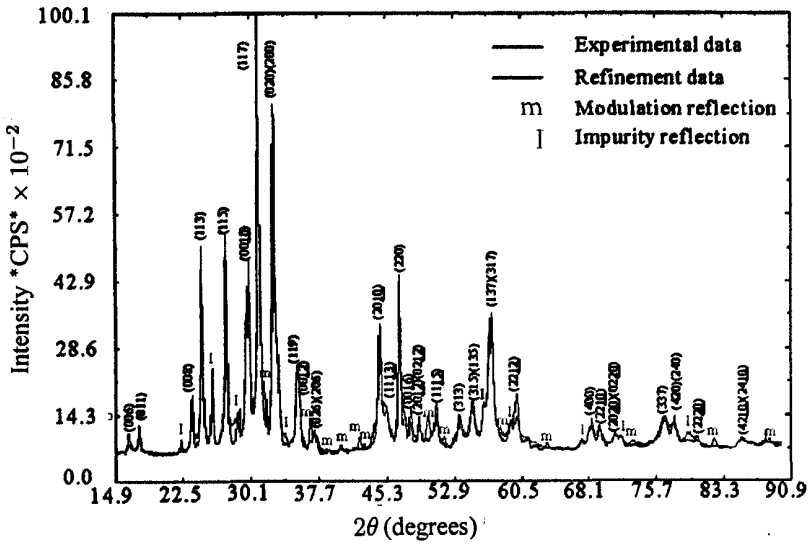

FIG. 2. X-ray difliaction pattern with peak index of main phase (Pr-doped Bi2212) labeled. Bold line is plotted with experimental points ($\theta/2\theta$ scan in $0.01^\circ/0.02^\circ$ step). Thin line is the calculated curve take into account the contribution of Pr-doped Bi22 12, Bi2201, Bi_2O_3 and SrO_2 phases.

TABLE II.

Weight Percentage (%) of Each Phase in the Bulk Sample	
$Bi_2Sr_2PrCu_2O_y$ (Pr-doped Bi2212)	67.30 ± 3.40
$Bi_2Sr_2CuO_6$ (Bi2201)	24.29 ± 4.73
Bi_2O_3 (Bismuth oxide)	0.52 ± 0.09
SrO_2 (Strontium oxide)	7.89 ± 0.69

With space group $Amaa$ and using the structure parameters of $Bi_2Sr_2CaCu_2O_{8+\delta}$ as the initial values, the unit cell parameter are calculated to be **a** $= 5.487(1)$, **b** $= 5.507(1)$, **c** $= 30.328(4)$Å, after the least squares fitting to the powder diffraction pattern. These results are closed to those obtained from the oscillation and Weissenberg photographs, using single crystal obtained from TSFZ method.

Rietveld analysis with RIQAS program package [10] shows the bulk sample obtained by the above process are still contaminated with impurity phases. The weight fractions of the main and impurity phases are listed in Table II.

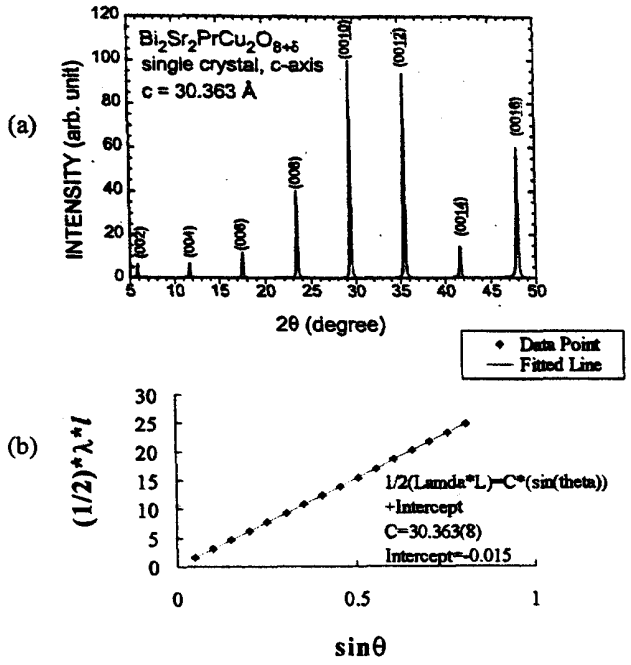

FIG. 3. (a) Diffraction patterns of $\theta/2\theta$ scan of a single crystal along **c**-axis, using a crystal of size $\sim 5 \times 4 \times 0.04$ mm^3 with **ab** plane on a low background quartz plate (6° off cut the (0002) plane). (b) Plot of $(\lambda/2 \bullet l)$ vs. sinθ for determination of **c**-axial length.

Single crystal of size $\sim 5 \times 4 \times 0.04$ mm^3 can be obtained, using traveling solvent floating zone method. The diffraction pattern of $\theta/2\theta$ scan along the *c*-axis of the crystal sample are shown in Fig. 3. No appreciable impurity peaks can be detected. Plane GIXD scan along (H00), (0K0) and (2K0) directions have been carried out. The scanning patterns, intensity versus H and K in relative lattice unit, are plotted in Fig. 4. The modulated peaks are 0.241(1) reciprocal lattice unit separated from the main peak along $\mathbf{b}^{\square}$-axis. This is approximately corresponding to 4.17-fold incommensurate super lattice in **b**-axis.

II-2. Single crystal X-ray diffraction collected by Weissenberg method

Using high intensity synchrotron X-ray in Photon factory and Weissenberg camera constructed therein [18, 20, 21, 22]. A single crstal of size $0.2 \times 0.1 \times 0.02$ mm^3 was selected and the shortest **a**-axis was aligned along the goniometer z-axis with the help of oscillation photograph (Fig. 5(a) and Fig. 5(b)). Then Weissenberg photograph was taken. The time of exposure for data collection can be accomplished within a few ten minutes. Fuji BASIII-type imaging plate, sensitivity 400 and BAS2000 IP reader were used for data collection. After preliminary investigation of the data, the cylindrical camera coupling constant of $2^{\pm}$/mm and imaging plate of sensitivity 400 were chosen for data analysis, which will be discussed in the following.

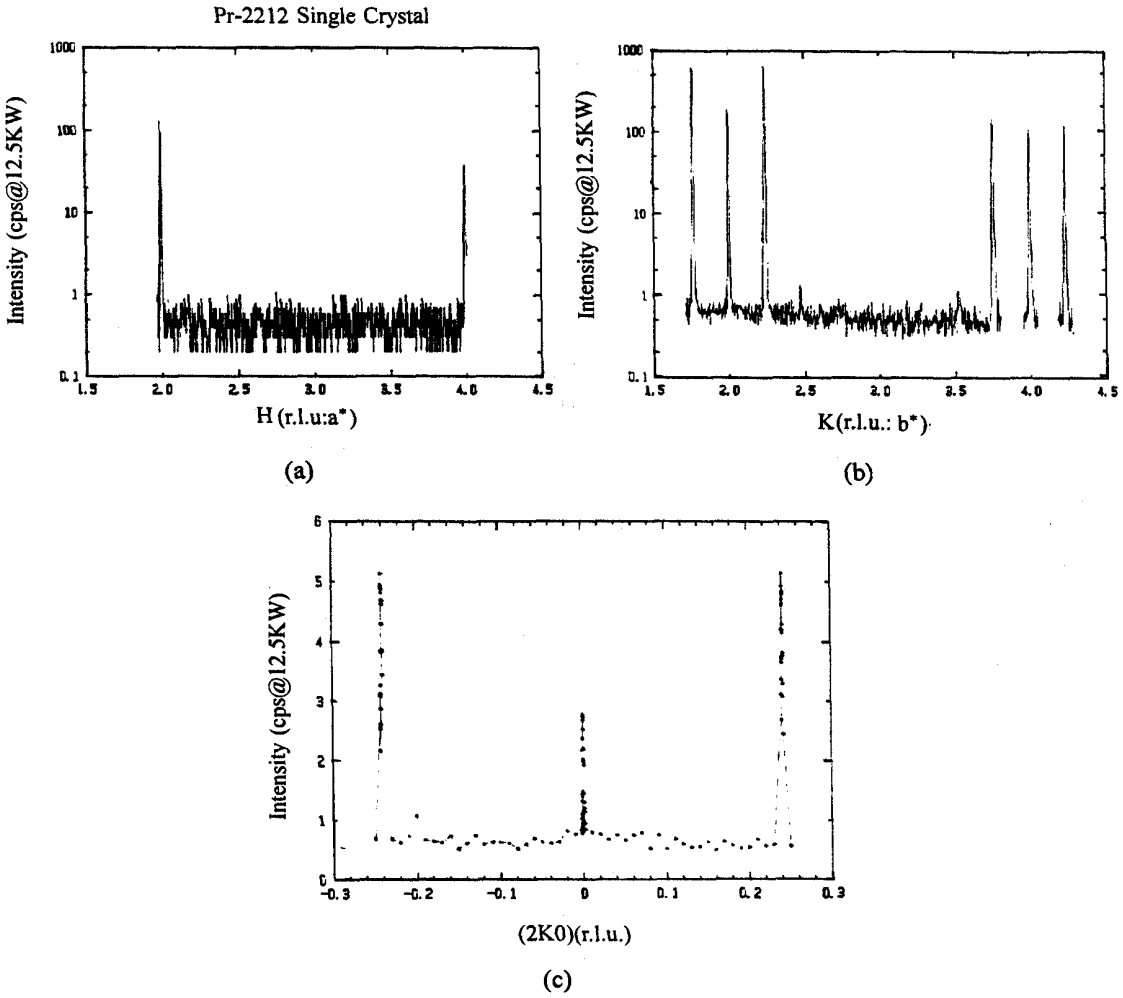

FIG. 4. Plane GIXD diffraction pattern of a small $Bi_2Sr_2PrCu_2O_{8+\delta}$ single crystal ($\sim 6 \times 4 \times 0.15$ mm^3 in size). (a) GIXD scan along (H00) direction. (b) GIXD scan along (0K0) direction. (c) GIXD scan along (2K0) direction.

III. Result and discussion

III-1. Determination for modulation wave vector q

A modulation wave is defined in reciprocal space by a "wave vector" **q**:

$$\mathbf{q} = \alpha \mathbf{a}^{\square} + \beta \mathbf{b}^{\square} + \gamma \mathbf{c}^{\square}$$

In this section, we would like to discuss how to determine the parameters, α, β, and γ for the modulation wave vector **q** from the satellites appear on the Weissenberg picture.

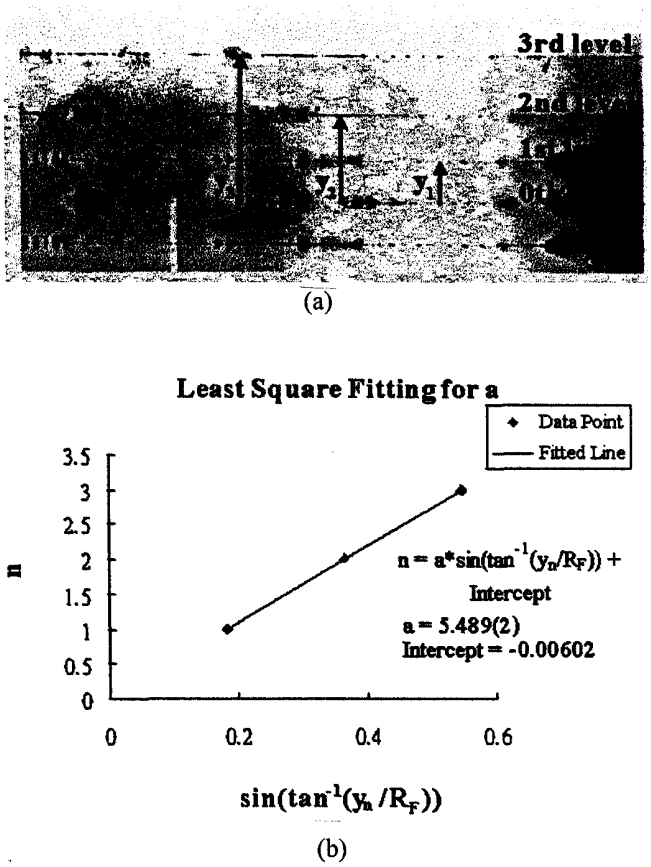

FIG. 5. Oscillation photographs (a) Scan range of $\omega : 0° \sim 15°$. (b) Plot of n vs. sin(tan^{-1} (y_n/R_F)) for determination of **a**-axial length.

For one-dimensionally modulated structure, the scattering vector **Q** is the sum of the scattering vector **H** and a multiple of the wave vector **q**:

$$\mathbf{Q} = \mathbf{H} + m\mathbf{q} = h\mathbf{a}^{¤} + k\mathbf{b}^{¤} + l\mathbf{c} * + m\mathbf{q}$$

Therefore, a quadruple index $(h, k, 1, m)$ is used to index a reflection plane in a modulated structure and the distance $d^{¤}$ of the reciprocal lattice point $(h, k, 1, m)$ from the origin is equal to $|h\mathbf{a}^{¤} + k\mathbf{b}^{¤} + l\mathbf{c}^{¤} + m\mathbf{q}|$. If orthorhombic symmetry is assumed for the crystal, then

$$(d^{¤})^2 = |\mathbf{Q}|^2 = (h + m\alpha)^2(\mathbf{a}^{¤})^2 + (k + m\beta)^2(\mathbf{b}^{¤})^2 + (l + m\gamma)^2(\mathbf{c}^{¤})^2$$

If the rotation axis is assumed to be **a**-axis, then we can only estimate the β and γ for the modulation wave vector **q** from the Weissenberg picture. For simplicity, we assume that the quadruple index (h, k, l, m) for any satellite reflection is known. Two satellites P_1, and P_2, which satisfy conditions $h_{P1} = h_{P2} = h$, $k_{P1} = k_{P2} = k$, $l_{P1} = l_{P2} + n$ (n is an integer) and

TABLE III. Structural parameters of $Bi_2Sr_2PrCu_2O_{8+\delta}$ obtain by Rietveld Refinement:

Temperature	300K		
Space group	A m a a	Z=1	
Crystal data	Mr=989.1957	Dx=7.633 /cm^3	
	F(000)=		
Cell parameter	a=5.487(2)Å	V=916.5Å^3	
	b=5.507(2)Å		
	c=30.33(1)Å		

Atom	Position	x	y	z	Occupancy
Pr	4c	0	0.25	0.25	1
Sr(1)	4c	0	0.25	0.25	1
Cu	8l	0	0.7562	0.1909	1
Sr(2)	8l	0	0.2648	0.1343	1
Bi	8l	0	0.7736	0.0501	1
O(1)	8h	0.25	0	0.2068	1
O(2)	8h	0.25	0.5	0.2068	1
O(3)	8l	0	0.8424	0.1298	1
O(4)	8l	0	0.18	0.0642	1
O(5)	8h	0.25	0	0.0454	0.125
O(6)	8h	0.25	0.5	0.0454	0.125

R values: R_{wp}=11.31, R_p=0.95%, R=12.72%
Crystallite size: 239.9(A) @2th=60.0 deg (Debye-Scherrer)
Preferred orientation vector = (0, 0, 1)
Preferred orientation parameter(s)= 0.0314 0

Selected inter-atomic distances (Å) and angles (degrees)

Bond	Dist (Å)	Bond	Angle
Pr-O(1)	2.344(3)	O(4)-Bi-O(3)	166.9(1)
Pr-O(2)	2.344(3)	O(4)-Bi-O(4)	159.4(1)
Cu-O(3)	1.913(2)	Bi-O(4)-Bi	159.4(1)
Cu-O(1)	1.979(2)		
Cu-O(2)	2.026(2)		
Sr-O(4)	2.177(2)		
Sr-O(3)	2.330(3)		
Bi-O(5)	1.859(2)		
Bi-O(6)	2.043(2)		
Bi-O(4)	2.279(3)		
Bi-O(3)	2.447(4)		

$m_{P1} = m_{P2} = m$, are chosen. Then,

$$(d^{\text{¤}}_{P1})^2 - (d^{\text{¤}}_{P2})^2 = (l_{P1} + m\gamma)^2(\mathbf{c}^{\text{¤}})^2 - (l_{P2} + m\gamma)^2(\mathbf{c}^{\text{¤}})^2$$

γ can be obtained after rearrangement,

$$\gamma = [(d^{\text{¤}}_{P1})^2 - (d^{\text{¤}}_{P2})^2 - (2nl_{P2} + n^2)(\mathbf{c}^{\text{¤}})^2]/2mn(\mathbf{c}^{\text{¤}})^2 \quad (1)$$

Similarly,

$$\beta = [(d^{\text{¤}}_{P1})^2 - (d^{\text{¤}}_{P2})^2 - (2nk_{P2} + n^2)(\mathbf{b}^{\text{¤}})^2]/2mn(\mathbf{b}^{\text{¤}})^2 \quad (2)$$

Another group of Weissenberg photographs must be taken with **b** or **c** as the rotating axis. In the similar way, α is as follows,

$$\alpha = [(d^{\text{¤}}_{P1})^2 - (d^{\text{¤}}_{P2})^2 - (2nh_{P2} + n^2)(\mathbf{a}^{\text{¤}})^2]/2mn(\mathbf{a}^{\text{¤}})^2$$

III-2. Determination of a-axial length from oscillation photograph

In the first step, oscillation photographs were customarily taken in order to align the crystal, so that the X-ray beam is normal to the rotation axis. However, which axis must the crystal be rotated about? From the studies of the incommensurate modulated structure, the Bi-based compounds were reported to have a structural modulation along the $\mathbf{b}^{\text{¤}}$ and $\mathbf{c}^{\text{¤}}$-axes in space group $Amaa$ (no. 66). Consequently, the crystal must be rotated about **a**-axis in order to observe the modulation reflections, which are expected to appear in the $\mathbf{b}^{\text{¤}}\mathbf{c}^{\text{¤}}$ plane.

Data collection was carried out under the conditions listed in Table IV.

TABLE IV.

Oscillation Image	
Energy and beam intensity of electron	3GeV, 168 ∼ 166 mA (BL6A)
X-ray wavelength	1.0A
Cylindrical cassette radius	143.25 mm
Diameter of beam slit	0.2×0.2 mm^2
Crystal Size	$0.2 \times 0.2 \times 0.02$ mm^3
Effective IP area	20×40 cm^2
Oscillation range	15 degree/frame
Coupling constant	0 degree/mm
Overlapping	0 degree
Exposure time	15 sec
Total frame number	12 (0 degree – 180 degree)

The oscillation images are shown in Fig. 5. Because of the similarity, we only show oscillation images from $0^{\pm} \sim 30^{\pm}$. Measuring y_n from Fig. 5(a), we can compute the length of rotation axis **a** as follows,

$$\begin{aligned} \mathbf{a} &= \frac{n\lambda}{\sin(\tan^{i\ 1}(y_n/R_F))} \\ n\lambda &= \mathbf{a}\sin(\tan^{i\ 1}(y_n/R_F)). \end{aligned}$$

For $\lambda = 1$Å and $R_F = 143.25$ mm,

$$n = \mathbf{a}\sin(\tan^{i\ 1}(y_n/143.25)).$$

By least square fitting (Fig. 5c), we get $\mathbf{a} = 5.489(2)$Å.

III-3. Determination of b- and c-axial length from Weissenberg photographs

A set of Weissenberg images were collected with coupling constant of $2^{\pm}$/mm and the conditions for this data collection are listed in Table V.

Fig. 6 shows the zero-level Weissenberg photograph. From the $0k0$ and $00l$ reflection spots, such as indicated in Fig. 6, we can detertnine the lattice parameters **b** and **c** by the following equation.

$$d_n^{\square} = 2\sin(y_n/2R_F).$$

TABLE V.

Weissenberg Image	
Energy and beam intensity of electron	3GeV, 165 mA(BL6A)
X-ray wavelength	1.0Å
Cylindrical cassette radius	143.25 mm
Diameter of beam slit	0.2×0.2 mm^2
Crystal Size	$0.2 \times 0.2 \times 0.02$ mm^3
Effective IP area	20×40 cm^2
Oscillation range	50 degree/frame
Coupling constant	2 degree/mm
Overlapping	0 degree
Exposure time	250 sec
Total frame number	4 (0 degree – 200 degree)

For the reflection spots on $0k0$,

$$k\mathbf{b}^{\ddagger} = d_k^{\ddagger} = 2\sin(y_k/2R_F).$$

For the reflection spots on $00l$,

$$l\mathbf{c}^{\ddagger} = d_l^{\ddagger} = 2\sin(y_l/2R_F).$$

By least squares calculation, we obtain $\mathbf{b} = 5.526(5)$Å and $\mathbf{c} = 30.42(7)$Å.

FIG. 6. (a) Zero-level Weissenberg photograph (b) The corresponding first-level Weissenberg photograph.

III-4. Determination of modulation wave vector q

In Fig. 7 (or Fig. 6), satellites reflection lines around **b**¤-axis can be clearly displayed up to 3rd-order $(m = 3)$ satellite reflections, which are not shown clearly in previous studies. The enlarged picture of these satellite diffraction peaks are shown in Fig. 7 for (0,2,0,m) and (0,4,0,m) "zone" lines. On the other hand, we found that the peak intensities of some of these satellites are as strong as the intensities of main reflections. May be the IP is over exposed, so that the recording of the high intensity main reflections reached saturation state. In any case, we can easily determine the modulation wave vector **q** with the pattern (refer to Fig. 9) in reciprocal space, which is obtained by transformation of the diffraction pattern in Fig. 6.

For the main reflections, we can easily index them. Actually, they are just equal to the coordinates in 3-dimensional reciprocal space. For the satellite reflections, the coordinates in this 3-D space are not integer, thus quadruple indices are used to index them. With m and modulation wave vector **q** indicated in Fig. 7, we can decide the quadruple index (h, k, l, m) for each satellite peak. For example, P_1 is a main reflection with index $(h_{P1},\ k_{P1},\ l_{P1},\ 0)$, then the indices for P_2 and P_3 are $(h_{P1},\ k_{P1},\ l_{P1},\ 1)$ and $(h_{P1},\ k_{P1},\ l_{P1},\ 2)$.

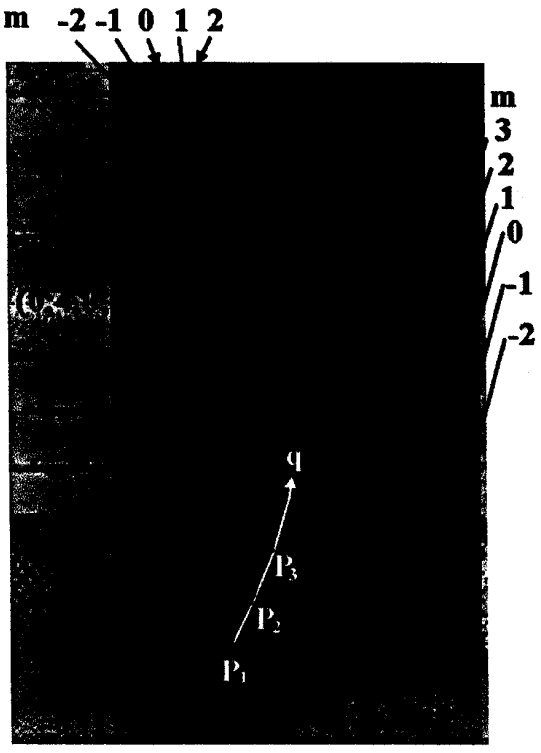

FIG. 7. Enlargement of zero-level Weissenberg photograph around (0, 2, 0, 0) and (0, 4, 0, 0) to show clearly the satellite reflections around the $\mathbf{b}^*$-axix $(0k0)$. Diffuse scattering of some diffraction points can be observed clearly.

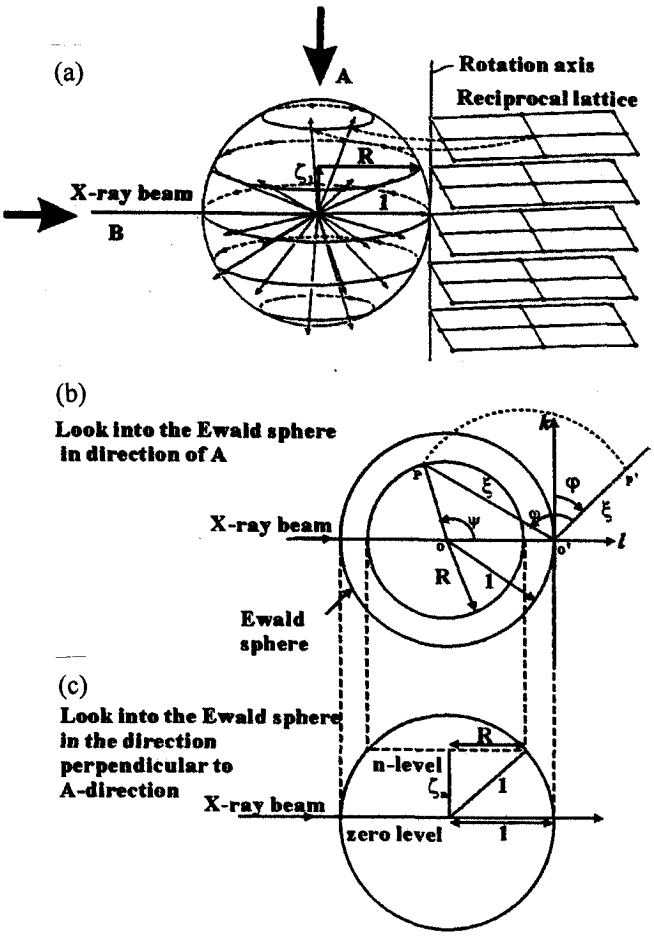

FIG. 8. Schematic diagram showing how the reciprocal lattice points come across the Ewald's sphere, give rise to Bragg diffraction points as they rotates around an axis.

As soon as the index of each satellite reflection is known, the parameters of **q** can be computed by equation (1) and (2). First, we estimate γ, the modulation along $\mathbf{c}^{\ast}$-axis, by least square calculation with the following relation:

$$\gamma = [(d^{\ast}_{P1})^2 - (d^{\ast}_{P2})^2 - (2nl_{P2} + n^2)(\mathbf{c}^{\ast})^2]/2mn(\mathbf{c}^{\ast})^2$$
$$\Rightarrow 2mn(\mathbf{c}^{\ast})^2\gamma = (d^{\ast}_{P1})^2 - (d^{\ast}_{P2})^2 - (2nl_{P2} + n^2)(\mathbf{c}^{\ast})^2$$

where $d^{\ast} = 2\sin(y/2R_F)$ and we get $\gamma \approx 1$. According to the report of some research works of one-dimensionally modulation in $Bi_2Sr_2CaCu_2O_{8+\delta}$ [15], γ is equal to 1, hence γ is set to 1. In addition, since it is well known that the Bi-based compounds have incommensurate modulation along $\mathbf{b}^{\ast}$ and $\mathbf{c}^{\ast}$-axis only, therefore, we only need to estimate the amount of modulation along $\mathbf{b}^{\ast}$ direction.

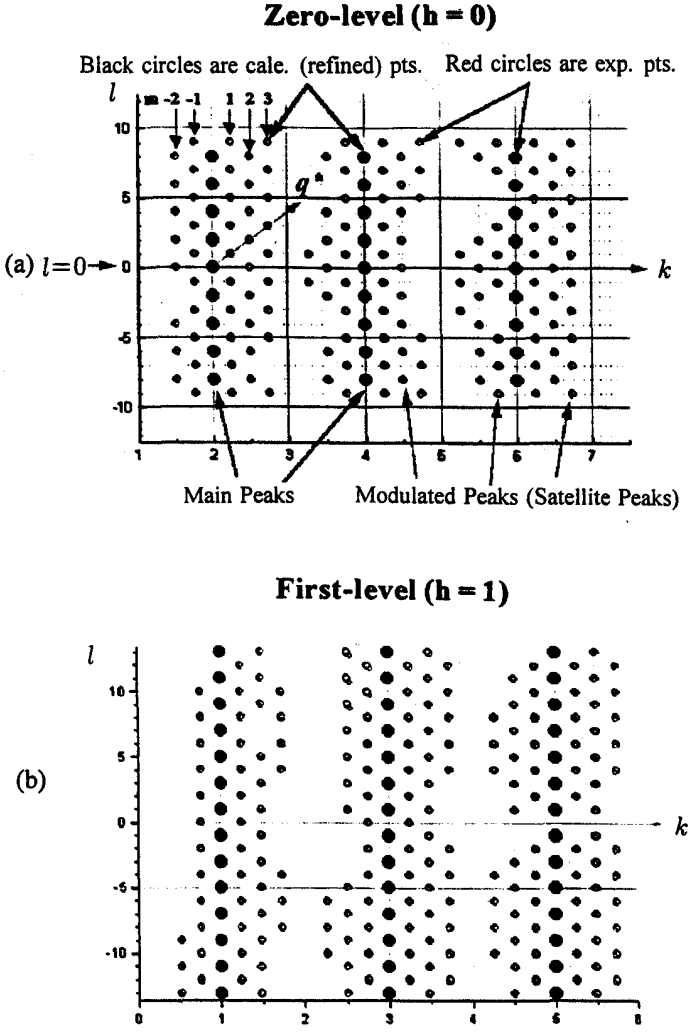

FIG. 9. Plot of reflection points in reciprocal lattice space. The larger circles are the main reflections; smaller circles are the satellite reflections. m is the fourth component of scattering vector $\mathbf{Q}(h,k,l,m)$.

By equation (2),

$$\beta = [(d^{*}_{P1})^2 - (d^{*}_{P2})^2 - (2nk_{P2} + n^2)(\mathbf{b}^{*})^2]/2mn(\mathbf{b}^{*})^2$$
$$\Rightarrow 2mn(\mathbf{b}^{*})^2\beta = (d^{*}_{P1})^2 - (d^{*}_{P2})^2 - (2nk_{P2} + n^2)(\mathbf{b}^{*})^2.$$

By least squares calculation, we get $\beta = 0.243\,(2)$. And the modulation wave vector is determined as,

$$\mathbf{q} = 0.243\mathbf{b}^{*} + \mathbf{c}^{*}.$$

This means that this $Bi_2Sr_2PrCu_2O_{8+\delta}$ single crystal has incommensurate modulation in **b** direction with period $\sim (1/0.243)$**b** and commensurate modulation in c direction.

III-5. Transformation from Weissenberg photograph to reciprocal space

From the principle of Weissenberg photograph [2], we can simply transform the film coordinate (x, y) to the angular coordinate (ω, ψ) by the two instrumental constant C_1, which is related to the radius R_F of the Weissenberg camera, and C_2, which is depended on the coupling of film translation to crystal rotation. The relation between (x, y) and (ω, ψ) are stated as follows,

$$\psi = C_1 y$$

$$= \frac{360^{\pm}}{2\pi R_F}\, y \text{ (in degree)}$$

$$= \frac{y}{R_F} \qquad \text{(in radian)}$$

$$\omega = C_2 x$$

In the following, we shall outline the relationship between (ξ, φ), the polar coordinate of a point in the reciprocal lattice space, and $\omega, \psi)$.

The n-level is normal to the rotation axis at a distance, ξ_n, above the zero-level. The n-level cuts the sphere of reflection in the reflecting circle for that level. The radius, R, of this circle is evidently given by, Fig. 8c,

$$R = \sqrt{1 - \xi_n^2}$$

If the rotation axis is **a**-axis, then $\xi_n = n\mathbf{a}^{\text{¤}}$.

The relation between the quantities involved is illustrated in Fig. 8b, by the law of cosines,

$$\xi^2 = 1 + R^2 - 2R\cos\psi \tag{3}$$

$$\varphi = \omega - (90^{\pm} - OO'P). \tag{4}$$

By the law of sines,

$$\angle OO^{\emptyset}P = \sin^{i\ 1}[(R/\xi)\sin\psi]. \tag{5}$$

Therefore,

$$\varphi = \omega - (90^{\pm} - \sin^{i\ 1}[(R/\xi)\sin\psi]). \tag{6}$$

As a conclusion, for a given (ξ, φ) in n-level, we can first get ψ by equation (3), and then get ω from equation (6). Alternatively, if (ω, ψ) within n-level are given, then we can first get ξ by equation (3), and then φ can be computed from equation (6).

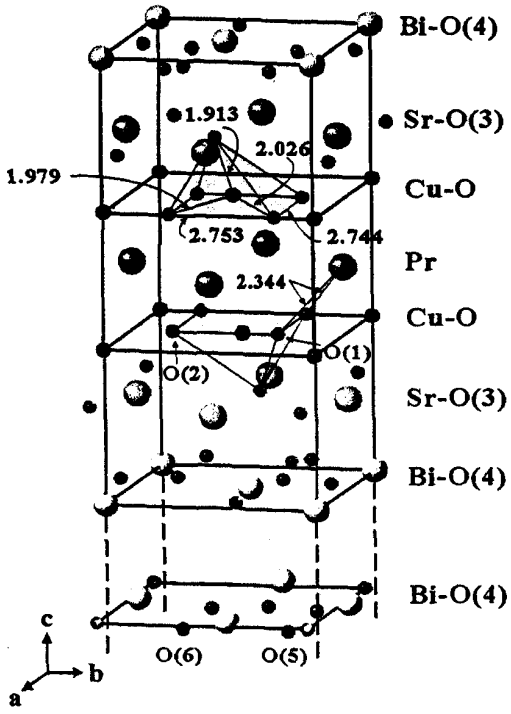

FIG. 10. Plot of the crystal structure for $Bi_2Sr_2PrCu_2O_y$ molecules in half unit cell (c/2). O5 and O6 are the extra oxygen atoms accounted for the modulation suggested. (Plotted with **Diamond** graphic program package).

For zero-level, $R = 1$, therefore,

$$\xi^2 = 2 - 2\cos\psi$$

$$= 2(1 - cos\psi)$$

$$= 4\sin^2(\psi/2)$$

$$\xi = 2\sin(\psi/2) \text{ (Bragg's law).}$$

In fact, ξ is equal to $d^{\square}$ in zero-level. From equation (5),

$$\sin(\angle OO^{\emptyset}P) = \frac{1}{\xi}\sin\psi$$
$$= \frac{1}{2}\frac{\sin\psi}{\sin(\psi/2)}$$
$$2\sin(\angle OO`P)\sin(\psi/2) = \sin\psi$$
$$= 2\sin(\psi/2)\cos(\psi/2)$$
$$\sin(\angle OO`P) = \cos(\psi/2)$$
$$\angle OO`P = 90^{\pm} - \psi/2$$

Therefore, from equation (4),

$$\varphi = \omega - (90^{\pm} - \angle OO^{\emptyset}P)$$
$$= \omega - (90^{\pm} - 90^{\pm} + \psi/2)$$
$$= \omega - \psi/2.$$

We can transform every reflection spot in zero-level, Fig. 6, to $k-l$ space by the definitions,

$$k = \xi\cos\varphi/\mathbf{b}^{\square}$$
$$l = \xi\sin\varphi/\mathbf{c}^{\square}.$$

The transformation of zero-level and first-level reflection points from Weissenberg photograph to $k-l$ space are shown in Fig. 9.

IV. Conclusion

We have found that the incommensurate modulated structures of $Bi_2Sr_2PrCu_2O_{8+\delta}$ in bulk and single crystal samples, there are the 3rd order satellite reflection spots in the Weissenberg photograph.

By the X-ray diffraction, we determine the space group of $Bi_2Sr_2PrCu_2O_{8+\delta}$ crystal to be orthorhombic $Amaa$ with cell parameters:

$$\mathbf{a} = 5.487(1) \quad \mathbf{b} = 5.507(1) \quad \mathbf{c} = 30.328(4).$$

And from the oscillation photographs and Weissenberg photographs, the lattice parameters **a**, **b**, **c** and modulation wave vector **q** are determined as follows,

$$\mathbf{a} = 5.489(2)\ \mathbf{b} = 5.526(7)\ \mathbf{c} = 30.420(5)\ \mathbf{q} = 0.243(2)\mathbf{b}^{\square} + \mathbf{c}^{\square}$$

In fact, this is a part in a series of studies between Prof. Noriyoshi Sakabe and us, with the help of Prof. Fan Hai-Fu in Chinese Academy of Science. We supply the crystal sample and Professor Sakabe collects the diffraction data for us and we try to read out intensity data. With

the help of Prof. Fan, we are going to determine the structure parameters of one-dimensionally incommensurate modulated structures by automatic search on 4-dimensional Fourier maps. Thus we expect to build a structure model according to the resultant Fourier map.

The Fourier maps can be obtained in the following steps:

1. Measuring the intensities of the reflections and obtained the $(h, k, 1, m, I)$ tables.

2. The phases of the structure factors for the main reflections can be derived by direct method, using the first modified Sayer equation list below,

$$F_m(h) =\approx \frac{\theta}{V}\sum_H F_m(h)F_m(h-h^0).$$

And a second modified Sayer equation below will be used to derive the phases of the satellites,

$$F_s(h) = \frac{\theta}{V}\left\{2\sum_H F_s(h)F_s(h-h^0) + \sum_H F_s(h)F_s(h-h^0)\right\}$$

where F_m and F_s are respectively structure factors of main and satellite reflections [30].

3. Calculate the 4-dimensional structure factor F according to the following expression,

$$F(\mathbf{h}_S) = \int d\bar{x}_4 \sum_{(\mathbf{R}j\tau)}\sum_{\mu} m^{\mu} f^{\mu} P^{\mu} \exp\left[-\sum_{i=1}^{4}\sum_{j=1}^{4} h_i(\mathbf{R}\mathbf{B}^{\mu}\tilde{\mathbf{R}})_{ij}h_j + i2\pi \mathsf{h}_S\cdot(\mathbf{R}\mathbf{x}+\tau)\right]$$

where $\mathbf{h}_S$, with components h_1, h_2, h_3 and h_4, is the position vector of a given 4-dimensional reciprocal lattice point. μ denotes the μ^{th} independent atom in the 4-dimensional unit cell. $\mathbf{R}$ and τ are respectively the rotation matrix and translation vector of the 4-dimensional space group symmetry operation. m^{μ} is the order of the symmetry operation, f^{μ} is the atomic scattering factor, P^{μ} is the occupancy and $\mathbf{B}^{\mu}$ is the anisotropic temperature-factor tensor of the μ^{th} atom. $\tilde{\mathbf{R}}$ is the transpose of $\mathbf{R}$.

4. The electron density in the (3+n)-dimensional space is obtained from the usual formula:

$$\rho(x_1,\ldots,x_{3+n}) = \frac{1}{V}\sum_{h_1\ldots h_{3+n}} F_{h^0}\exp\left\{2\pi i\sum_{j=1}^{3+n} h_j x_j\right\}$$

where V is the volume of the fundamental cell in R_3 and $h_1,\ldots,h_{3+n}$ run over all integers [27].

5. Plot the electron density distribution map (the 4-dimensional Fourier maps).

6. Build up the structure model according to Fourier maps determined in step 4.

7. Perform the LSQ refinement for the atomic parameters, using the model build in step 5, then construct the Difference Fourier maps to obtain the position of lighter atoms, then do the LSQ calculation again.

Finally, we will get the refined structure model, close to the real one.

Acknowledgments

This work was supported by the National Science Council of the Republic of China under Contract No. NSC88-2212-M007-004, NSC88-2212-M007-052.

References

[1] A. I. Beskrovnyi *et al*., Physica C **206**, 27-32 (1993).
[2] M. J. Buerger, *X-Ray Crystallography*, (John Weiley & Sons, New York, 1962) p. 221-251.
[3] P. M. De Wolff *et al*., Acta Cryst. A **37**, 625 (1981).
[4] Z. Q. Fu *et al*., Ultramicroscopy **54**, 229 (1994).
[5] K. K. Fung *et al*., J. Phys. (Cond.) **1**, 317 (1989).
[6] Y. Gao *et al*., Physica C **160**, 431 (1989).
[7] Y. Gao, Materials Science Forum **100**, 237 (1992).
[8] R. E. Gladyshevskii and R. Flukiger, Acta Cryst. B **52**, 38 (1996).
[9] E. A. Hewat *et al*., Physica C **153**, 619 (1988).
[10] Jade and Ruby are program package for search, match and structure identification from XRD powder patterns. RIQAS is a system for the analysis of X-ray and neutron powder diffraction data employing Rietveld and whole-pattern fitting. Copyright by Material Data, Inc., Livermore, CA 94550 USA, (925) 449-1048. E-mail address: mdi@materialsdata.com
[11] A. Janner and T. Janssen, Phys. Rev. B **15**, 643 (1977).
[12] A. Janner, T. Janssen and P. M. De Wolff, Acta Cryst. A **39**, 658 (1983).
[13] T. Jansen *et al*., International Tables for Crystallography, Kluwer Academic Publishers, Dordecht, **797**, 843 (1992).
[14] X. B. Kan and S. C. Moss, Acta Cryst. B **48**, 122 (1992).
[15] J. Q. Li *et al*., Z. Phys. B (Coed) **74**, 165 (1989).
[16] H. Meada *et al*., Jpn. J. Appl. Phys. **27**, L209 (1988).
[17] P. A. Miles *et al*., Physica C **294**, 275 (1998).
[18] Y. Noda *et al*., J. Synchrotron Rad. **5**, 485 (1998).
[19] V. Petricek *et al*., Phys. Rev. B **42**, 387 (1990).
[20] K. Sakabe *et al*., J. Synchrotron Rad. **4**, 136 (1997).
[21] N. Sakabe *et al*., Rev. Sci. Instrum. **66** (2), February (1995).
[22] N. Sakabe, Nucl. Instrum. Methods **A303**, 448 (1991).
[23] M. A. Subramanian *et al*., Science **239**, 1015 (1988).
[24] X. F. Sun *et al*., Physica C **295**, 218 (1998).
[25] X. F. Sun *et al*., Physica C **305**, 227 (1998).
[26] X. F. Sun *et al*., Physica C **307**, 67 (1998).
[27] J. M. Tarascon *et al*., Phys. Rev. B **37**, 9382 (1988).
[28] A. Yamamoto, Acta Cryst. A **38**, 87 (1982).
[29] A. Yamamoto *et al*., Phys. Rev. B **42**, 4228 (1990).
[30] Q. Hao, Y. W. Liu & H. F. Fan, Acta Crryst. A **43**, 820 (1987).
[31] Li. Yang, Z. H. Wan, H. F. Fan, *MIMS–A program for measuring 4-dimensional Fourier maps of incommensurate modulated structures*, (Chinese Academy of Sciences, Beijing, 1999).